Optica Applicata, Vol. XXII, No. 3–4, 1992

High speed response of GaAs/AlGaAs multiple quantum well asymmetric Fabry–Perot reflection modulator

M. NAWAZ

Institute of Physics, Electronics Group, University of Oslo, Boks 1048 Blindern, 0316 Oslo, Norway.

B. T. OLSEN, K. MCILVANEY

Norwegian Telecom Research P.O. Box 83. N–2007, Kjeller, Norway.

The results of the high speed response of GaAs/AlGaAs multiple quantum well (MQW) based on asymmetric Fabry–Perot (ASFP) reflection modulator are presented. The measured 3 dB electrical frequency reponse bandwidth of the modulator was 600 MHz at an applied voltage of only 5 V at 854 nm wavelength. The contrast ratio of the modulator was 8.9 dB for a driving voltage of 13 V, at an operating wavelength of 862 nm.

1. Introduction

During the last few years, high speed external modulators based on semiconductor quantum well structures have been studied extensively. These include both waveguide modulators [1], in which the light propagates in the plane of the quantum well layers, and surface normal reflection modulators [2], which allow the perpendicular illumination of the light to the quantum well layers. The MQW based modulators enhance shifts of the absorption edge due to excitonic properties toward a longer wavelength (*i.e.* red shift) as an external electric field is applied perpendicular to the quantum well layers, a phenomena called the quantum confined Stark effect (QCSE), [3]. The reflection modulators have the advantage of improving the modulation contrast over transmission [4] modulators, by a double pass [2] of the incident light through the quantum wells and are considered as promising candidates for implementing two dimensional arrays for optical interconnections of integrated circuits and optical computing applications [5], [6].

A Fabry–Perot cavity [7], [8] modulator is formed by the introduction of highly reflecting layers (multiple quarter wavelength stacks) on both sides of the MQW structure, to increase the optical path length (and thus contrast ratio) more than simple reflection modulators [2]. To implement the asymmetric Fabry–Perot cavity, unequal mirrors are used. The asymmetric Fabry–Perot modulators have been proposed [8], [9] to provide both low insertion losses and high contrast ratios, with suitable optical bandwidths. The principle of operation of ASFP

modulators is as follows: without cavity loss, the overall reflectivity is quite high (*i.e.* on state) if the bottom mirror reflectivity is made close to unity and the top mirror reflectivity is significantly less. With applied fields, the increased cavity loss reduces the effective reflectivity from the bottom mirror at the top surface, and the effective reflectivity from the bottom mirror has an equal magnitude to the top mirror reflectivity, yielding the off state. In principle, this will result in a high contrast ratio (theoretically infinity) at lower operating voltages. Among various important issues in the design of the ASFP structure is the need to achieve high speed of response. Various high speed modulators [2], [10] using GaAs/AlGaAs MQW system, which usually operates at about ~850 nm have been demonstrated, but little or no attention has been drawn to the high speed of response of the ASFP modulators. In this paper, we present the high speed performance of an asymmetric Fabry–Perot reflection modulator with GaAs/AlGaAs MQW as an active region. The measured 3 dB electrical frequency response bandwidth of the modulator was 600 MHz, with a drive voltage of only 5 V, at an operating wavelength of 854 nm. The measured contrast ratio of the modulator was 8.9 dB for a driving voltage of 13 V, at a wavelength of 862 nm, with a very low insertion loss of ~3 dB.

2. Device layer structure

The modulator layer structure was grown by molecular beam epitaxy (MBE) at Delab in Trondheim (Norway). It consists of 1 μm n-doped buffer layer grown on the n-doped GaAs substrate, followed by a dielectric mirror design consisting of 20 periods of 2.83 Å n-type AlAs and 25.44 Å n-type GaAs. Over this are 75 undoped multiple quantum wells (MQW) consisting of a 96.11 Å GaAs well between 59.38 Å AlGaAs barriers. On top of this, is the 250 Å undoped AlGaAs buffer layer, followed by p-doped 4556 Å AlGaAs layer, and finally, there are two cap layers of 10 Å and 40 Å p-doped GaAs to complete the PIN diode structure. For n-type doping, Si was used with doping concentration $\sim 1 \times 10^{18}\,\mathrm{cm}^{-3}$, while Be was used for p-type doping concentration $\sim 1 \times 10^{18}\,\mathrm{cm}^{-3}$. All AlGaAs layers in the structure contain 30% of Al. The buffer layer was used to separate the intrinsic region from any background doping diffusion. The semiconductor–air interface forms

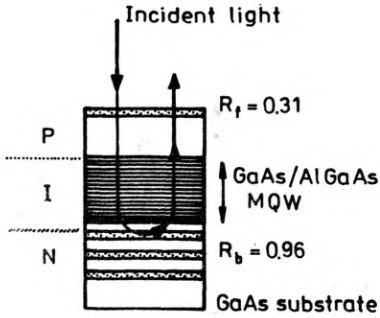

Fig. 1. Schematic cross-section of the ASFP reflection modulator with front mirror reflectivity (semiconductor–air interface) $R_f = 0.31$, and back mirrors reflectivity (dielectric stacks) $R_b = 0.96$

the front mirror, whose reflectivity is 0.31, while dielectric stacks grown on the n-doped GaAs substrate form the back mirror, whose reflectivity is 0.96. The structure is like an asymmetric Fabry–Perot cavity, because of unequal front and bottom mirror reflectivities. The device was prepared by etching mesas of 220 μm circular diameter, connected to a contact pad of 100 μm squared. The Au metal was evaporated onto the sample as p-ohmic contact and Au/Ge/Au/Ni/Au as n-ohmic contact. Figure 1 shows a schematic cross-section of the ASFP reflection modulator.

3. Experiment

To test the quality of the PIN diode modulator, I–V measurements were first performed without illumination of the light, using HP 4145B semiconductor parameter analyser. The reverse breakdown voltage of the device was −25 V and a dark current of 4.3 and 10 nA was measured under a reverse bias voltage of −5 and −10 V, respectively. The device was connected to the microstrip transmission line through the Au bonded wire, whose length was ~5 mm. The reflection spectra of the modulator were measured using a white light source in the spectral range from 830 to 900 nm. The directional coupler (Gould 136193) attached to it, 1 meter long multimode fiber at both ends, was used to couple light from the light source and perpendicular incident onto the sample. The wavelength resolution was improved using 0.1 mm slit, placed in front of the monochromator (Jobin Yvon H10) interfaced with a computer system. The reflected signal from the modulator was detected using HP 81530A power sensor, set at a wavelength of 850 nm, and the data values were recorded in the digital form. The reverse DC bias perpendicular to the quantum well layers was applied at the input of the transmission line from the Øltronix power supply (86000). To eliminate the effects of variations in the measurement system response with wavelengths, the background noise signal was first measured and subtracted from the actual measured values of the reflected signal, and the result was normalized using the reference signal. All these measurements were performed at room temperature.

The speed of response of the modulator was measured in the frequency domain because of convenience. An AlGaAs laser diode was used as a light source for the perpendicular illumination of light onto sample. The incident light was 11 mW, and set at a wavelength of ~854 nm. The modulator was driven by an RF signal from the signal generator with an upper limit of 2.7 GHz, applied at the input of the transmission line through a bias T, where a reverse DC bias of −5 V was superimposed. The RF signal was 1 and 2 V pp (peak to peak). The reflected signal was detected by an HP 83410A receiver and its output was connected to the spectrum analyser to observe the measured frequency response. The frequency responses of the receiver, the cables, and the bias T were separately calibrated to enhance the accuracy of measurements. The calculated capacitance of the device was 4.8 pF, for 1.16 μm thick MQW region with an area of 4.799×10^4 μm^2 of the device.

4. Results and discussion

The results of the reflection spectra are plotted and presented in Figure 2, with and without bias. The position of the light hole (lh) and heavy hole (hh) excitons at zero bias is marked at ~842 and ~848.4 nm, respectively. The Fabry–Perot (FP) mode is also indicated at ~860 nm. An FP mode is defined as the wavelength at which the

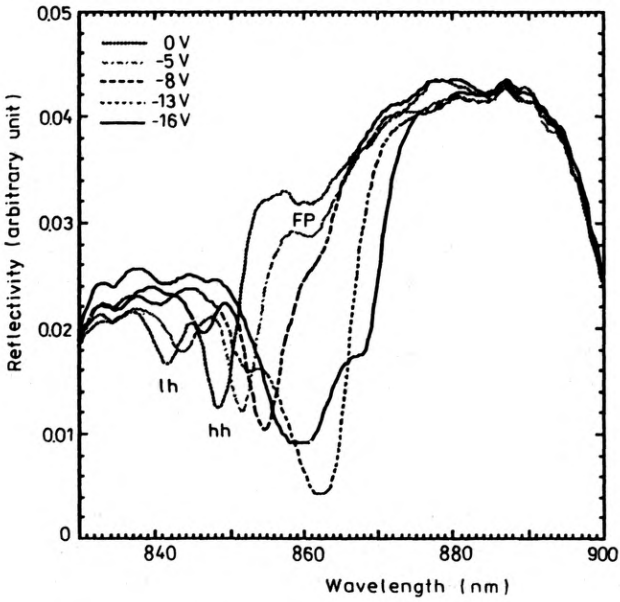

Fig 2. Reflectivity spectra at different reverse biases

net reflectivity of the losses cavity is maximum. The mode position depends on the cavity length as well as the refractive index. The measured FWHM (full width half maximum) of the hh exciton was ~4 nm which tells about the quality of the material used. The separation of the zero bias hh exciton from the FP mode was ~11.6 nm. The zero bias separation between the exciton (hh) and the FP resonance wavelength effects both the initial value of the reflectivity at the FP wavelength and the ability to redshift the exciton with applied bias to achieve a minimum in reflectivity due to the increased loss in the cavity. The net reflectivity of the ASFP modulator decreases with applied reverse biases, reaches its minimum value (where the cavity is matched) at −13 V, and then increases again because of decreased absorption in the MQW region due to the QCSE [3]. The lh and hh excitons shift their position towards higher wavelengths (*i.e.* redshift) with increasing reverse bias. However, the lh exciton broadens and looses its oscillator strength more rapidly than the hh exciton. The hh hole exciton is well resolved, and coincides with the FP mode at the Fabry–Perot resonance at −13 V. Once the hh exciton passes the FP mode, it reappears towards higher wavelength with increasing bias (*i.e.* at −16 V). The measured energy shift of

the hh exciton at different reverse biases is in good agreement with the theoretical energy shift [11]. The theoretical and experimental results of the hh exciton energy shift are compared and presented elsewhere [12]. The measured contrast ratio (defined as the ratio of maximum reflectivity at zero bias to the reflectivity under certain reverse bias) was about 8.9 dB for a reverse bias of −13 V, at an optimum wavelength of 862 nm as shown in Fig. 3. The measured contrast ratio of the

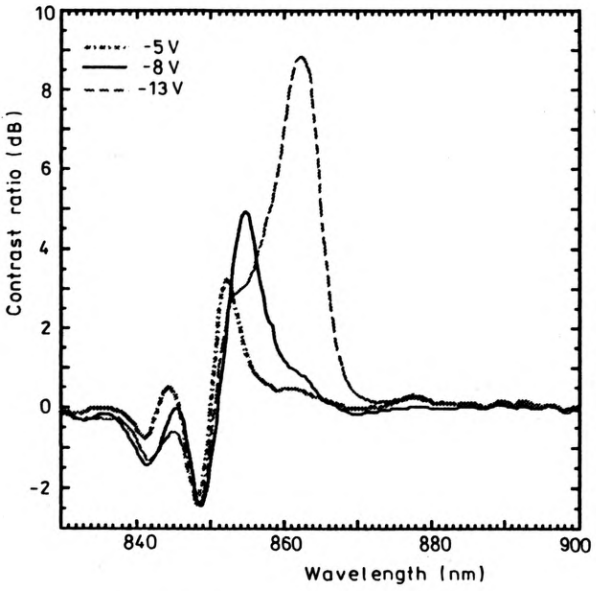

Fig. 3. Meaured contrast ratio as a function of wavelength

modulator was limited by the experimental setup and background noise which caused a severe reduction in the reflectivity measurements. The insertion loss of the device was experimentally determined to be equal 3 dB at 862 nm. These results are encouraging for the subsequent development of ASFP modulators [7], [8] for high contrast ratios with low insertion loss.

To determine the suitability of the device for the speed response measurements, the return loss of the device was first measured (using swept network analyser, HP 8702A), without illumination of the light, and plotted in Fig. 4. The frequency scan was from 300 KHz to 3 GHz. The return loss of the device is insensitive (as expected) of the frequency. However, a small resonance of −5 dB at 450 MHz was observed in the return loss due to the mismatched impedance of the device and the transmission line. The results of the frequency response for a reverse bias of 5 V, and at a wavelength of 854 nm are plotted and presented in Fig. 5. The measured contrast ratio for a reverse bias of 5 V was ~2.1 dB at 854 nm. We decided to drive the modulator at lower voltage (*i.e.* 5 V) that can run at similar energy densities to good electronic devices (*e.g.* present TTL system). For the integration of MQW modula-

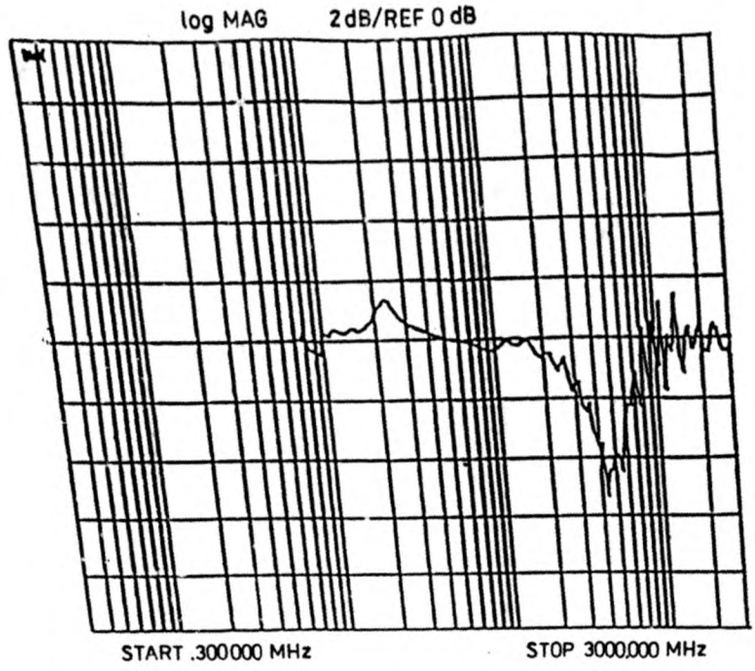

Fig. 4. Return loss measurement of the device

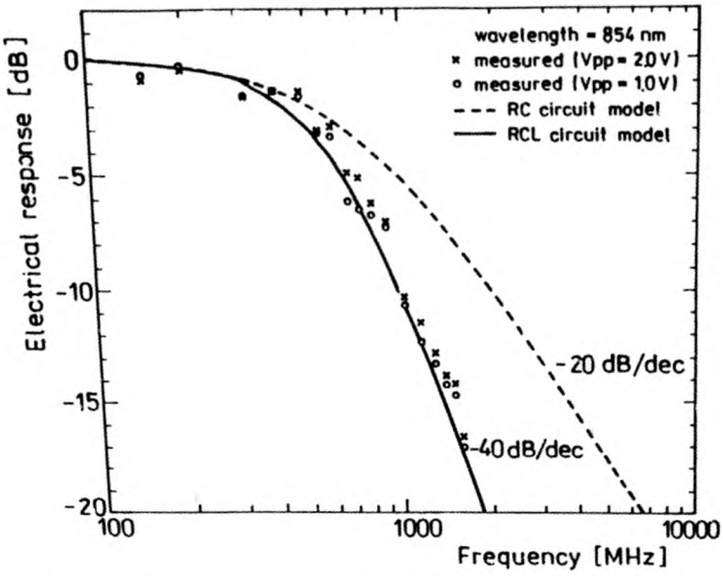

Fig. 5. Measured and calculated frequency response of the modulator

tors with VLSI circuits as optical interconnectors a significantly lower operating voltage is desirable. The measured 3 dB electrical frequency response bandwidth of the modulator was 600 MHz. The frequency response bandwidth was independent of the driving voltage (*i.e.* 1 and 2 V_{pp}). If the modulator is modelled as a simple *RC* series circuit in which the response is proportional to the voltage across the capacitor (Fig. 6), then the frequency response is given by:

$$FR(\text{dB}) = -10 \log \left[1+\left(\frac{f}{f_c}\right)^2\right], \tag{1}$$

$$f_c = 1/2\pi RC \tag{2}$$

where R is the source resistance (50 ohm) and C is the capacitance (4.8 pF) of the device. The response of this equivalent circuit model is also plotted in Fig. 5. The measured 3 dB electrical frequency response bandwidth is in excellent agreement with the frequency response bandwidth of the equivalent circuit model. However,

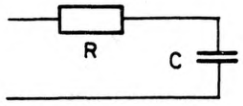

Fig. 6. Equivalent circuit of the modulator

the slope of the measured frequency response drops rapidly at higher frequencies than that of the calculated frequency response from the equivalent circuit model. This rapid drop in the slope of the measured frequency respose is due to the excess voltage drop across the inductance associated with the long bonding wire, which resulted in the reduction in the voltage drop across the capacitance of the device. To justify this, we have modelled a new RLC series circuit (Fig. 7), where L is the

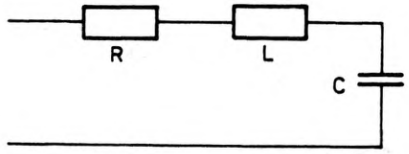

Fig. 7. New circuit model for the frequency response

inductance of the bonding wire, R is the source resistance and C is the capacitance of the device.

The frequency response of the new circuit model is

$$FR(\text{dB}) = -10 \log\left[\left(1-\left(\frac{w}{w_0}\right)\right)^2 + \frac{R^2C}{L}\left(\frac{w}{w_0}\right)^2\right], \tag{3}$$

$$w_0 = \frac{1}{\sqrt{LC}}. \tag{4}$$

The best fit of the simulated frequency response from the new circuit model (*i.e.* RLC) is also plotted in Fig. 5. The best fit was obtained using $R = 50\ \Omega$, $C = 4.8$ pF, $L = 7.7$ nH. However, the inductance of the bonding wire used in the simulations is ~58% higher than calculated inductance of ~4.5 nH from the theory [13]. The decay in the measured and simulated frequency response is ~ -40 db/dec at higher frequencies. Since the response of the material to the applied field variation is very fast [14] (*i.e.* < 1 ps) and also the measurement system used in this work has a speed of response much faster than the device speed, therefore the electrical frequency response bandwidth is limited by the circuit considerations such as the

capacitance of the device and the inductance of the long bonding wire. The inductance of the bonding wire can be reduced by using short bonding wire [15] (*i.e.* < 1 mm). The capacitance of the device can be made small by minimizing the device area, increasing the thickness of the intrinsic region and using a relatively thick ploymide layer under the contact pad [15]. Using these considerations, the speed of the device can be increased further, which is the object of future research.

Acknowledgements – This research work was carried out at Norwegian Telecom Research (NTR), P. O. Box 83. N–2007, Kjeller, Norway. The authors are grateful to P. I. Jensen and G. Salmonson, for designing and K. Johansen, for growing the modulator layer structure. We are also thankful to T. Olsen for fruitful discussions and suggestions during this work.

References

[1] KOTAKA I., WAKITA K., MITOMI O., ASAI H., KAWAMURA Y., IEEE Photon Technol. Lett. 1 (1989), 100.
[2] BOYD G. D., BOWERS J. E., SOCCOLICH C. E., MILLER D. A. B., CHEMLA D. S., CHIROVSKY L. M. F., GOSSARD A. C., ENGLISH J. H., Electron. Lett. 25 (1989), 558.
[3] MILLER D. A. B., CHEMLA D. S., DAMEN T. C., GOSSARD A. C., WIEGMANN W., WOOD T. H., BURRUS C. A., Phys. Rev. B 32 (1985), 1043.
[4] STEVENS P. J., PARRY G., J. Lightwave Technol. 7 (1989), 1101.
[5] WOOD T. H., J. Lightwave Technol. 6 (1988), 743.
[6] SIMES R. J., YAN R. H., GEELS R. S., COLDREN L. A., ENGLISH J. H., GOSSARD A. C., PARRY G., Electron Lett. 53 (1988), 637.
[7] YAN R. H., SIMES R. J., COLDREN L. A., Appl. Phys. Lett. 55 (1989), 1946.
[8] YAN R. H., SIMES R. J., COLDREN L. A., IEEE J. Quantum Electron. 27 (1991), 1922.
[9] BUYDENS L., DEMEESTER P., VAN DAELE P., Opt. Quantum Electron. 24 (1992), S167.
[10] WOOD T. H., BURRUS C. A., MILLER D. A. B., CHEMLA D. S., DAMEN T. C., GOSSARD A. C., WIEGMANN W., IEEE J. Quantum Electron. QE 21 (1985), 117.
[11] MCILVANEY K., Ph. D. Thesis, Department of Electrical Engineering, Glasgow, University, Scottland, 1990.
[12] NAWAZ M., M. Sc. Thesis, Institute of Physics, University of Oslo, Norway, 1992.
[13] MEINKE H., GUNDLACH F. W., *Taschenbuch der Hochfrequenztechnik*, Springer-Verlag, 1976, p. 14.
[14] SCHMITT RINK S., CHEMLA D. S., KNOX W. H., MILLER D. A. B., Opt. Lett. 15 (1990), 60.
[15] MITOMI O., KOTAKA I., NOJIMA S., KAWANO K., KAWAMURA Y., ASAI H., Appl. Opt. 31 (1992), 2030.

Received March 11, 1993